Minimization of background correction errors using nonlinear estimates of the changing background in carbon furnace atomic absorption spectrometry

ARTICLE *in* ANALYTICAL CHEMISTRY · NOVEMBER 1986

Impact Factor: 5.64 · DOI: 10.1021/ac00126a006

2 AUTHORS:

James A Holcombe
University of Texas at Austin
167 PUBLICATIONS **2,837** CITATIONS
SEE PROFILE

James Harnly
Agricultural Research Service
163 PUBLICATIONS **3,397** CITATIONS
SEE PROFILE

by 1-2 orders of magnitude, especially for chromium(III). Because chromium(III), titanium, iron(III), and aluminum are unstable in the neutral and alkaline pH region, these elements are concentrated at pH 3-4. Although some foreign ions (Mg^{2+}, Mn^{2+}, and Al^{3+}) interfere with chromium(III) determination in this technique, the low detecion limit for chromium(III) provides an application of this technique to clinical and environmental samples.

ACKNOWLEDGMENT

The authors express their thanks to T. Kumamaru, Faculty of Science, Hiroshima University, for his helpful discussion on this work.

Registry No. Al, 7429-90-5; Cr, 7440-47-3; Fe, 7439-89-6; Ti, 7440-32-6; V, 7440-62-2.

LITERATURE CITED

(1) Olsen, S.; Pessenda, L. C. R.; Růžička, J.; Hansen, E. H. *Analyst (London)* **1983**, *108*, 905.
(2) Kamson, O. F.; Townshend, A. *Anal. Chim. Acta* **1983**, *155*, 253.
(3) Fang, Z.; Růžička, J.; Hansen, E. *Anal. Chim. Acta* **1984**, *164*, 23.
(4) Malamas, F.; Bengtsson, M.; Johansson, G. *Anal. Chim. Acta* **1984**, *160*, 1.
(5) Fang, Z.; Xu, S.; Zhang, S. *Anal. Chim. Acta* **1984**, *164*, 41.
(6) Hirata, S.; Umezaki, Y.; Ikeda, M. *Bunseki Kagaku* **1986**, *35*, 106.
(7) Hartenstein, S. D.; Růžička, J.; Christian, G. D. *Anal. Chem.* **1985**, *57*, 21.
(8) McLeod, C. W.; Cook, J. G.; Worsfold, P. J.; Davies, J. E.; Queay, J. *Spectrochim. Acta, Part B* **1985**, *40B*, 57.
(9) Cox, A. G.; Cook, L.G.; McLeod, C.W. *Analyst (London)* **1985**, *110*, 331.
(10) Kumamaru, T.; Matsuo, H.; Okamoto, Y.; Ikeda, M. *Anal. Chim. Acta* **1986**, *180*, 171.
(11) Cambell, P. G. C.; Bisson, M.; Bougie, R.; Tessier, A.; Villeneuve, J. P. *Anal. Chem.* **1983**, *55*, 2246.
(12) Leyden, D. E.; Underwood, A. L. *J. Phys. Chem.* **1964**, *68*, 2093.
(13) Sides, J. L.; Kenner, C. T. *Anal. Chem.* **1986**, *38*, 707.
(14) Kingston, H. M.; Barnes, I. L.; Brady, T. J.; Rains, T. C., Champ, M. A. *Anal. Chem.* **1978**, *50*, 2064.
(15) Florence, T. M. *Anal. Chim. Acta* **1982**, *141*, 73.
(16) Sillen, L. G.; Martell, A. E. *Stability Constants*; The Chemical Society: London, 1964; Special Publications No. 17.
(17) Wing, R. K.; Peterson, V. J.; Fassel, V. A. *Appl. Spectrosc.* **1979**, *33*, 206.
(18) Swaidan, H. M.; Christian, G. D. *Anal. Chem.* **1984**, *56*, 120.

RECEIVED for review February 20, 1986. Accepted June 24, 1986.

Minimization of Background Correction Errors Using Nonlinear Estimates of the Changing Background in Carbon Furnace Atomic Absorption Spectrometry

James A. Holcombe

Department of Chemistry, University of Texas at Austin, Austin, Texas 78712

James M. Harnly*

USDA, Nutrient Composition Laboratory, Building 161, BARC—East, Beltsville, Maryland 20705

Nonsimultaneous measurement of the sample and background absorbance signals in electrothermal AAS can produce significant background correction errors. Interpolation between two background values (bracketing mode) gives a better estimate of the background value at the sampling point than is the case when a single measurement of the background for correction (asymmetric mode) is used. The use of three or four background values fit to a quadratic equation provides additional improvement in the accuracy of background correction. The extent of improvement is dependent on the mathematical function that is descriptive of the background signal. The errors are shown to be proportional to the third and fourth derivative of the actual function for a three- and four-point fit, respectively. Computer simulations of the expected errors as well as experimental verification using an oscillating refractor plate to simulate background fluctuations are presented. A 2% NaCl sample was used to generate a background signal, which was then treated using the four distinct modes of correction.

Regardless of the method of background correction, significant errors arise from the nonsimultaneous measurement of the sample and reference signal. Harnly and Holcombe (*1*) have previously shown that the size of the error and the shape of the error function depend on the elapsed time, Δt, between the sample and reference measurements and the number of reference measurements employed in the absorbance computation. Traditionally, only a single reference measurement is used, either before or after the sample measurement. The error resulting from this *asymmetric* sampling mode is given by the product of the first derivative of the background absorbance function and Δt. If reference measurements made before and after the sample measurement are used in the absorbance computation, a linear interpolation is used to compute the reference value. This *bracketing* mode of computing absorbances produces errors that are equal to half the product of the second derivative of the background absorbance function and $(\Delta t)^2$. The maximum error using the bracketing mode is usually significantly less than the maximum asymmetric mode error.

A nonlinear interpolation of the reference value can be obtained by fitting a nonlinear equation to three or more of the reference values surrounding the sample measurement. While the asymmetric and bracketing mode assume no change and a linear change, respectively, in the background absorbance, a nonlinear interpolation will accommodate nonlinear changes in the background. In addition, use of more reference values will result in a more statistically accurate reference value computed for the time of the sample measurement. Like the asymmetric and bracketing modes, the nonlinear interpolation modes will produce a systematic error that must be determined and evaluated.

In this study, nonlinearly interpolated reference values will be computed from quadratic equations fit to three and four reference values bracketing the sample measurement. The

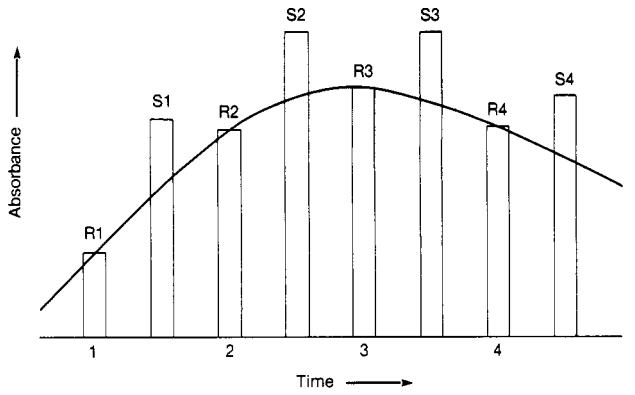

Figure 1. Repetitive sequential measurement of the reference (R) and sample (S) absorbances for the case of a constant atomic absorbance signal and changing background absorbance.

interpolation method of background correction will be compared to the asymmetric and bracketing modes with respect to minimizing background correction errors. The quadratic fits are achieved through the convolution of the reference values with a chosen set of coefficients as described by Savitsky and Golay (*2*). The error function of the quadratic equations applied to three and four reference values will be evaluated.

EXPERIMENTAL SECTION

Equipment. Data were acquired using a prototype continuum source spectrometer SIMAAC, which has been described previously (*3*). To simulate background absorption, a quartz plate mounted on a galvanometer (Model 6325 PD, General Scanning, Inc., Watertown, MA) was located in the position of the carbon furnace. Oscillation of the quartz plate produced varying degrees of reflection and refraction of the source beam, which appeared as source attenuation at the photomultiplier tube. The galvanometer was driven by a scanner controller (Model CCX101, General Scanning, Inc.). The sine wave used as the driving wave form was generated by a function generator (Model 901, Beckman Instruments, Inc., Richmond, CA).

Data Acquisition Program. Simplistically, SIMAAC acquires data in the absorbance domain at a frequency of 56 Hz; i.e., a reference and sample absorbance are obtained every 18 ms at 9-ms intervals (symmetrically alternating between the reference and sample measurements). The sample absorbance reflects the sample and the background absorbance, while the reference absorbance reflects only the background absorbance. Background-corrected absorbances are computed in four different ways. As shown in Figure 1, a block of eight sample (S1–S4) and reference (R1–R4) absorbances were treated at one time. For the asymmetric mode, background-corrected absorbance is computed as S2 – R2. For the bracketing mode, the corrected absorbance is S2 – [(R2 + R3)/2]. For the nonlinear interpolation modes using three and four reference points, quadratic equations are fit to the first three (R1–R3) and all four (R1–R4) reference absorbances, respectively. In each case, the interpolated reference absorbance, R_{Ref}, is computed for the time S2 is acquired and the corrected absorbance is computed as S2 – R_{Ref}. After completion of the computation of the four background-corrected absorbances, the first two values (R1 and S1) are dropped and the next two values (R5 and S5) are used to form a new block of eight sample and reference absorbances. After redefining the points (R2–R5 become R1–R4, and S2–S5 become S1–S4), the next set of four background-corrected absorbances is computed.

In reality, all data are acquired in the intensity domain. Each sample and reference value are the sum of 10 intensity measurements. Ideally, intensity values should be converted to absorbances before further processing. Summing data in the intensity domain before computing absorbances can lead to errors due to the nonlinearity of the intensity domain (*4*). The SIMAAC data acquisition program processes the data in the intensity domain to facilitate and expedite the calculations. It will be shown that differences in the background-corrected absorbances for the intensity and the absorbance domain are negligible.

Background Absorbance Model. A computer program was developed that used a mathematical model for the background absorbance (*1*) and simulated the data acquisition scheme of SIMAAC. This model is the linear transformation of a normal distribution in the logarithmic domain. The background absorbance was

$$A = b_1\{\exp[-[\ln (t/b_2)]^2]\} \quad (1)$$

where b_1 and b_2 are variables determining the amplitude and the width of the background signal and t is the time. The data acquisition and processing were modeled in two ways: in the intensity domain, exactly as SIMAAC acquires and processes the data, and in the absorbance domain, where every measured value was an absorbance and all processing occurred entirely in the absorbance domain. In both cases, background-corrected absorbances were computed using all four modes.

Background Simulation. Background was simulated by inserting an oscillating quartz plate in the source beam between the source and the carbon furnace. This produced only a background absorption with no atomic absorption present. Thus, any background-corrected absorbance that exceeded the range of the normal base-line absorbance noise was due to a systematic error in the background correction method. The repetitive nature of the oscillating quartz plate (unlike true background) permitted a statistical analysis (computation of standard deviation) of the errors.

Atomization of 2% NaCl. A solution of 2% NaCl was made up from a Specpure standard (Jarrell-Ash Co., Waltham, MA). A volume of 20 μL was atomized at 2700 °C from the wall of the furnace. An internal argon gas flow of 50 mL min^{-1} was used. Data were collected just off the Pb wavelength, 283.3 nm. Although no Pb was detectable in the NaCl, the quartz refractor plate was disengaged to ensure that no atomic absorption signal could influence the background-corrected absorbance tracings. Data were acquired and tracings were made as described above.

RESULTS AND DISCUSSION

Quadratic Least-Squares Fit. This discussion, for the sake of clarity, will consider all analytical measurements in the absorbance domain. Experimental data were processed in the intensity domain. Differences arising from the use of intensities in place of absorbances will be discussed later in the paper.

Every atomic absorption spectrometer makes a systematic series of absorbance measurements alternating between the sample and the reference signal (Figure 1). A least-squares fit of a quadratic equation to the reference values can be used to provide a nonlinearly interpolated reference value at the time of the sample measurement. Obviously, a set of three or more reference points that bracket the sample measurement can be chosen in a number of ways. For this study, two approaches were evaluated. The quadratic 3 mode used three reference measurements (R1–R3) with the sample measurement (S2) located between the second and third reference measurements, and the quadratic 4 mode used four reference measurements (R1–R4) with the sample (S2) located between the second and third reference measurements. While the time intervals between the sample and the preceding and trailing reference measurements may not be equal, the time interval between the reference measurements is constant. Thus, for a series of four consecutive reference measurements, the time coordinates can be designated as 1, 2, 3, and 4 with absorbances of A_1, A_2, A_3 and A_4, respectively, with the sample measurement of interest located between times 2 and 3.

A quadratic equation of the form

$$Y = b_0 + b_1X + b_2X^2 \quad (2)$$

where Y is the reference absorbance, X is the time, and b_0, b_1, and b_2 are the polynomial coefficients, can be fit to three or more points using the least-squares method. The sets of generalized coefficients that result from a matrix algebra solution to the least-squares fit are shown in Table I for three

Table I. Coefficients for eq 1 for n = 3 and 4

		coeff at given values of n			
n = 3	b_0	$(+3)A_1$	$(-3)A_2$	$(+1)A_3$	
	b_1	$(-5/2)A_1$	$(+4)A_2$	$(-3/2)A_3$	
	b_2	$(+1/2)A_1$	$(-1)A_2$	$(+1/2)A_3$	
n = 4	b_0	$(+9/4)A_1$	$(-3/4)A_2$	$(-5/4)A_3$	$(+3/4)A_4$
	b_1	$(-31/20)A_1$	$(+23/20)A_2$	$(-27/20)A_3$	$(-19/20)A_4$
	b_2	$(+1/4)A_1$	$(-1/4)A_2$	$(-1/4)A_3$	$(+1/4)A_4$

and four points (n = 3 and n = 4).

The nonlinearly interpolated reference value, A_{Ref}, is computed by substituting the values of b_0, b_1, b_2, and the time, X, of the sample measurement into eq 1. For n = 3 and the sample measured at time 2.5 (evenly spaced between reference measurements 2 and 3), eq 1 gives an interpolated reference value of

$$A_{ref,3} = (-A_1 + 6A_2 + 3A_3)/8 \tag{3}$$

For n = 4, the computed reference value is

$$A_{ref,4} = (-A_1 + 9A_2 + 9A_3 - A_4)/16 \tag{4}$$

The integer factors and the normalization constants, shown in eq 3 and 4, can be used to compute the interpolated reference absorbance for any set of three or four consecutive reference measurements when the sample is equidistant from the references. A different spacing of the sample between the reference values would produce different integer factors and normalization constants. These can be computed from eq 2 by inserting the appropriate X value for the sample measurement time.

Error Functions. The background-corrected absorbance, A_{NL}, using the nonlinear interpolation mode is

$$A_{NL} = A_S - A_{Ref} \tag{5}$$

where A_S is the measured sample absorbance. If no analytical atomic absorption occurs, then eq 5 will be a statement of the background correction error, E_{NL}. This expression can be further expanded using eq 3 and 4 for three and four reference measurements, respectively

$$E_{NL,3} = A_S - A_{Ref,3} = \frac{A_1 - 6A_2 + 8A_S - 3A_3}{8} \tag{6}$$

$$E_{NL,4} = A_S - A_{Ref,4} = \frac{A_1 - 9A_2 + 16A_S - 9A_3 + A_4}{16} \tag{7}$$

It was shown in a previous study (*1*) that systematic background correction errors arising from the asymmetric and bracketing modes of absorbance computation were proportional to the first and second derivatives, respectively, of the background absorbance function. It can be shown that the systematic errors for the quadratic 3 and quadratic 4 modes are proportional to the third and fourth derivatives, respectively, of the background absorbance function.

Consider, again, the case of four reference values A_1, A_2, A_3, and A_4 measured at times 1, 2, 3, and 4 and a sample value A_S measured at time 2.5. To define the time scale and facilitate the calculations, let the time interval of 0.5 correspond to Δt. Thus, in this case, Δt is the elapsed time between the sample and reference meausrements. Numerically, any two points can be used to compute a first derivative,

$$\frac{dA}{dt} = \lim_{\Delta t \to 0} \frac{f(t + \Delta t) - f(t)}{\Delta t} \tag{8}$$

or for the second reference and sample value

$$\frac{dA}{dt} = \frac{A_2 - A_S}{\Delta t} \tag{9}$$

Similarly, three points can be used to compute a second derivative, four points to compute a third derivative, and so on. The numerical expression of the third derivative (using reference values 1–3 and the sample value) is

$$\frac{d^3A}{dt^3} = \frac{A_1 - 6A_2 + 8A_S - 3A_3}{(15/4)\Delta t^3} \tag{10}$$

and the fourth derivative is

$$\frac{d^4A}{dt^4} = \frac{A_1 - 9A_2 + 16A_S - 9A_3 + A_4}{(75/16)\Delta t^4} \tag{11}$$

Combining eq 6 and 10 and eq 7 and 11 the error functions become

$$E_{NL,3} = (15/32)\ \Delta t^3 \frac{d^3A}{dt^3} \tag{12}$$

and

$$E_{NL,4} = (75/256)\ \Delta t^4 \frac{d^4A}{dt^4} \tag{13}$$

Equations 12 and 13 show that the systematic errors for the quadractic 3 and quadratic 4 modes are proportional to the third and fourth derivative, respectively, of the background absorbance function. Thus, for all four correction modes, the effect of lack of fit is predictable, but the exact shape and amplitude of the error functions are dependent on the background function. Unfortunately, there is no accurate model for the background or analytical absorbance function. The relative degree of error for all four modes can only be inferred from models, simulated background, or analytical data.

Background Absorbance Models. A mathematical model was previously used to illustrate the error functions (*1*). This model, a normal distribution function in the logarithmic domain (see Experimental *section*), approximates the time-dependent background signal (Figure 2A). By use of this model, data acquistion at a rate of 56 Hz was simulated on a computer. One sample and one reference measurement were made every 18 ms at 9-ms intervals. The data were used to compute background-corrected absorbances by manipulating the reference values in the four ways previously described (see Experimental Section). Since no atomic absorption was included in the modeling, the background correction errors were equal to the difference between the sample and the variously computed reference absorbances. The plots of the background correction errors as a function of time are shown in Figure 2.

The asymmetric, bracketing, quadratic 3 and quadratic 4 modes display classical first, second, third, and fourth derivative functions, respectively (Figure 2B–E). A comparison of the amplitude of the errors (note the change in the Y-axis scales) shows that the errors are significantly reduced as higher derivatives are used. For this model (and $b_1 = b_2 = 1$) the maximum error value for the quadratic 4 mode is ~7 times less than the quadratic 3 mode, which in turn is ~11 times less than the bracketing mode, which is ~44 times less than the asymmetric mode. Errors for each computation mode will decrease as Δt is decreased and as the sample measurement is shifted closer (temporally) to the reference measurement. However, the ranking of the modes with respect to the magnitude of the background correction error will remain the same.

Table II shows that the advantage of the higher derivatives decreases as the half-width decreases. The error ratio of the asymmetric and quadratic 4 modes is 3333 and 22 for peak widths of 1.85 and 0.23 s, respectively. The latter background signal is quite severe. Under these circumstances, however,

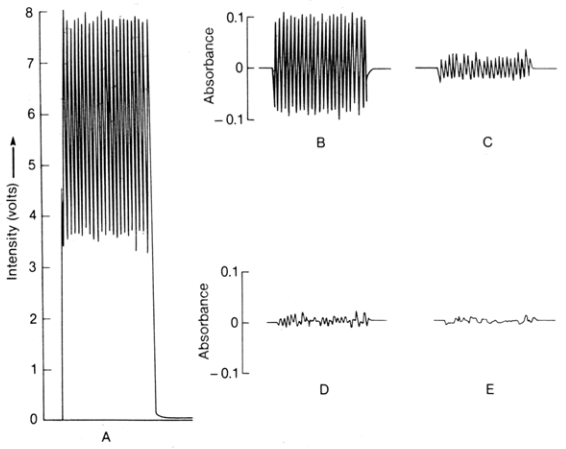

Figure 2. Computer-modeled background correction errors for (A) an absorbance model; $A = \exp[-(\ln t)^2]$ for the (B) asymmetric, (C) bracketing, (D) nonlinear (three points), and (E) nonlinear (four points) methods of absorbance computation.

Table II. Maximum and Minimum Errors for Background Absorbance Model[a] vs. Peak Width

	b_2 = 1.0	b_2 = 0.5	b_2 = 0.25	b_2 = 0.125
peak half-width(s)	1.85	0.92	0.46	0.23
asym[b]				
max. error	0.016 665	0.033 325	0.066 714	0.138 463
min. error	−0.003 936	−0.007 872	−0.015 725	−0.031 473
brack[c]				
max. error	0.000 376	0.001 504	0.006 051	0.026 614
min. error	−0.000 326	−0.001 281	−0.004 357	−0.008 844
quad (3)[d]				
max. error	0.000 035	0.000 223	0.001 160	0.007 341
min. error	−0.000 035	−0.000 273	−0.001 894	−0.007 079
quad (4)[e]				
max. error	0.000 005	0.000 042	0.000 582	0.006 359
min. error	−0.000 005	−0.000 067	−0.000 670	−0.002 601

[a] $A = b_1\{\exp[-[\ln (t/b_2)]^2]\}$, $b_1 = 1.0$. [b] Asymmetric mode. [c] Bracketing mode. [d] Quadratic (three points) mode. [e] Quadratic (four points) mode.

the quadratic 3 and quadratic 4 modes are both a factor of 4 better than the bracketing mode.

Two versions of the computer model were developed. In the first version, the results reported above were obtained by handling all the data in the absorbance domain. The sample and reference data were computed directly in absorbance units, and the data were handled as shown in eq 2–13. The second version processed the data in the intensity domain, the form in which the experimental data were acquired by the computer. The sample and reference intensity data can immediately be changed to absorbance data by using a stored reference intensity. However, a single modulation cycle of 10 sample and 10 reference measurements would require 20 divisions and 20 logarithmic determinations instead of only one each if the data are handled in the intensity domain.

In the intensity domain, the generalized eq 2–4 can be used by substituting $I_1 - I_4$, I_S, and I_{Ref} for $A_1 - A_4$, A_S, and A_{Ref}, respectively. Thus, intensity-dependent expressions for eq 5–7 are

$$A_{NL} = I_{Ref}/I_S \quad (14)$$

$$E_{NL,3} = I_{Ref,3}/I_S \quad (15)$$

$$E_{NL,4} = I_{Ref,4}/I_S \quad (16)$$

Handling the data in the intensity domain can lead to nonlinearities not found in the absorbance domain (*4*). However, the general shapes and magnitudes of the plots in Figure 2 are essentially unchanged when the data are handled in the intensity domain. A slight increase was observed for the maxima of the second and third peaks and a slight decrease in all the minima. The ratios of the maximum errors were unchanged from the results reported in the preceding paragraphs.

In general, the comparative errors from absorbance vs. intensity calculations are dependent on the nature of the function describing the reference points being fit. For example, a background whose intensity is changing linearly will show less error when the intensity domain calculation mode is used. The reverse is true if the background absorbance is changing linearly with time. Since there is presently no good analytical expression capable of accurately describing the time-dependent background signal, it is not obvious which mode should produce the minimum error in all cases.

Experimentally Simulated Background. The source intensity of an AAS was attenuated by using an oscillating quartz plate located in the position of the carbon furnace as described in the Experimental Sectior. During a complete cycle (using sine wave modulation), approximately 50% of the source intensity was attenuated (Figure 3A) thus simulating the rapid transient background absorption signals observed with furnace atomization. The frequency of the background absorption was easily controlled, but it was impossible to isolate a single cycle. Consequently, the simulated background absorption was repeated continuously over a data acquisition time of 10 s.

Figure 3 shows the source intensity and the absorbances (errors) computed using the four modes of background correction for background absorption at 10 Hz. The large noise amplitude and the cyclic nature of the noise for the asymmetric, bracketing, and quadratic 3 modes indicated systematic background correction errors.

Background absorbance errors at 10 Hz, using the present data collection frequencies, are close to a worst case example. At a frequency of 10 Hz with maximum and minimum intensities of 7.8 and 3.7, respectively, the maximum rate of absorbance change was 10.1 A s^{-1}. Background frequencies of 1, 2, and 5 Hz yielded maximum rates of 1.7, 3.1, and 6.8 A s^{-1}, respectively. The background attenuation decreased slightly with increased frequency as a result of decreased

Table III. Standard Deviation of the Background-Corrected Absorbance Errors[a]

simulated modulation frequency, Hz	source intensity, arbitrary units	absorbance computation modes[b]			
		asym	brack	nonlin (3)	nonlin (4)
0	8.3	0.0046	0.0043	0.0044	0.0044
0	2.4	0.0083	0.0076	0.0080	0.0079
1	2.3–8.3	0.0121	0.0054	0.0057	0.0056
2	2.6–8.3	0.0237	0.0058	0.0059	0.0058
5	3.1–8.3	0.0530	0.0108	0.0063	0.0054
10	3.7–7.8	0.0869	0.0254	0.0132	0.0083

[a] Background simulated by modulation of a quartz refractor plate in the source beam. [a] asym, asymmetric; brack, bracketing; nonlin (3), nonlinear (three points); nonlin (4), nonlinear (four points).

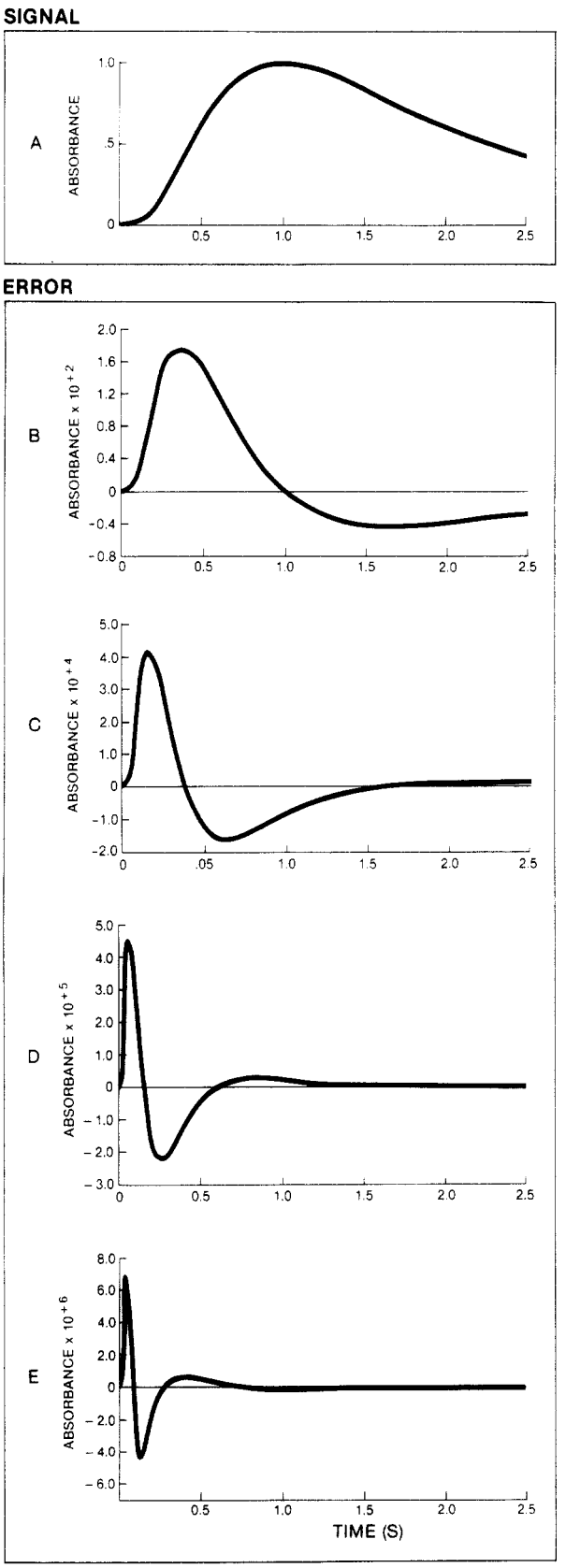

Figure 3. (A) Intensity vs. time profile for a 10-Hz sine wave simulated background. Background correction errors for the (B) asymmetric, (C) bracketing, (D) nonlinear (three points), and (E) nonlinear (four points) methods of absorbance computation.

modulation amplitude of the quartz reactor plate and produced the nonlinear change in the maximum rates. Grobenski et al. (5) reported absorbance changes of 3–5 A s^{-1} for seawater samples using atomization from a platform with the maximum

Table IV. Error Maxima and Minima for 2% NaCl[a]

absorbance computation mode	H_2O blank		2% NaCl	
	max	min	max	min
asymmetric	0.021	−0.016	0.098	−0.122
bracket	0.021	−0.015	0.025	−0.023
nonlinear (3 pts)	0.022	−0.017	0.023	−0.025
nonlinear (4 pts)	0.021	−0.016	0.023	−0.027

[a] 20 μL of 2% NaCl was atomized from the wall at 2700 °C with an internal argon flow of 50 mL min^{-1}. Data were collected at 283.3 nm. The absorbance data were not filtered.

heating rate. Absorbance changes as high as 10 A s^{-1} were reported for the worst conditions (5). Consequently, refractor plate modulation frequencies between 1 and 10 Hz exceed the rates of absorbance change expected for furnace atomization.

Quantification of the background correction errors can be accomplished by computing the standard deviation of the computed absorbances. In Table III, the standard deviations are shown for all four absorbance computation modes at modulation frequencies of 1, 2, 5, and 10 Hz as well as the standard deviations obtained at the maximum and minimum source intensities. With no transient background and the maximum source intensity (8.3), the standard deviation of the computed absorbances was 0.0044 (it must be remembered that these are unfiltered absorbances with a time constant of 18 ms). At the minimum intensity (2.4) the standard deviation was 0.0079. This is expected for a shot-noise-limited system, since the ratio of the noise levels, 0.0079/0.0044 = 1.80, is approximately equal to the square root of the intensity change ($(8.3/2.4)^{1/2}$ = 1.86). At the average intensity of 5.35, with no contribution from background correction errors, a standard deviation of 0.0055 would be predicted. It can be seen that all modes except the asymmetric mode gave this noise level at refractor plate frequencies of 1 and 2 Hz. At 5 Hz, only the quadratic 4 mode remained unperturbed. At 10 Hz the noise level for the quadratic 4 mode increased by 51% in comparison with 24%, 462%, and 1581% for the quadratic 3, bracketing, and asymmetric modes, respectively.

For this experiment, the data acquisition program handled the data in the intensity domain as described in the Experimental Section. By use of the computer model described in the previous section with a sine wave background signal, the difference between the absorbance and intensity domain was evaluated. If the data were handled in the absorbance domain, the noise levels in Table I would be unchanged for the asymmetric and the bracketing mode. For the nonlinear interpolation modes, the noise at 1 and 2 Hz would be decreased by 14% and 6%, respectively. Thus, handling the data in the intensity domain simplified the computation (i.e., 20 times fewer divisions and logarithm determinations) and had little impact on the size of the background correction error.

High Salt Sample. To illustrate the background correction errors expected for an actual sample, a solution of 2% NaCl was atomized using the conditions described in the Experimental Section. The results are shown in Figure 4 and Table IV. It must be emphasized that the absorbance tracings in Figure 4 are not filtered and have an effective time constant of 18 ms. Filtering the data would reduce the random baseline absorbance noise to a greater extent than the magnitude of the systematic background correction errors. Filtering would be more advantageous for the nonlinear fits as the higher derivatives have narrower maxima and minima (Figure 2).

The asymmetric and bracketing errors provide the maximum absorbances in Figure 4B,C. In Figure 4D,E, the systematic errors are less than the noise peak. The noise peak

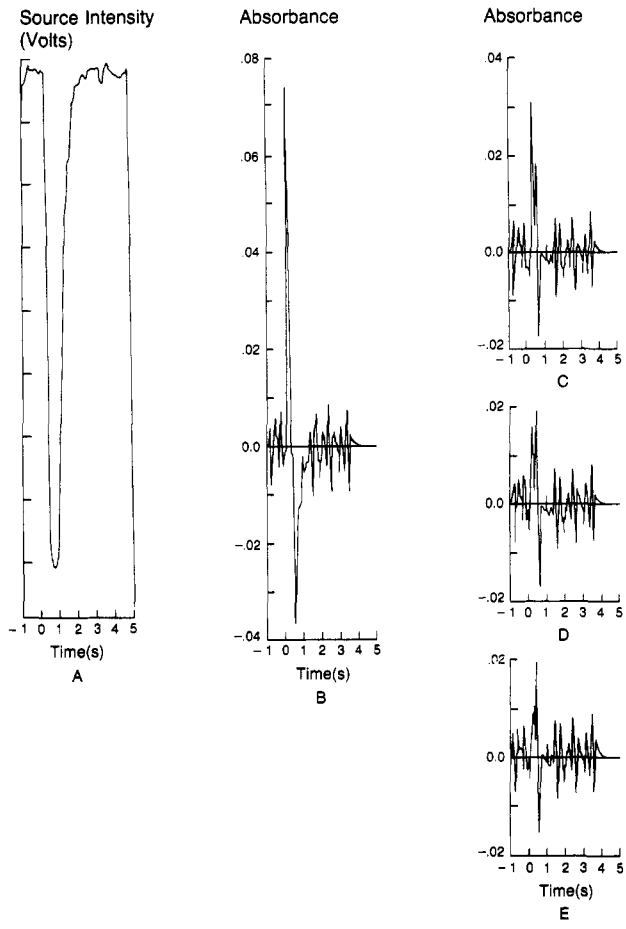

Figure 4. (A) Recorded intenstiy for the atomization of 2% NaCl. Background correction errors for the (B) asymmetric, (C) bracketing, (D) nonlinear (three points), and (E) nonlinear (four points) methods of absorbance computation.

is easily seen in Figure 4C–E and arises from the increased base-line absorbance noise that accompanies the loss of source intensity. The loss of a factor of 9 of source intensity (Figure 4A) would produce a 3-fold ($9^{1/2}$) increase in the base-line noise for a shot-noise-limited system. Thus, the noise peak in Figure 4 is well within the expected limits.

The magnitudes of the systematic errors shown in Figure 4B–E are dependent on all of the factors that influence the shape of the background absorption signal (heating rate, internal gas flow rate, sample size, wavelength, and atomization from wall or platform) and the time interval between the sample and reference measurements. The signal in Figure 4A was acquired using a modest sample size (20 μL), a fairly high internal flow rate (50 mL min^{-1}), and determined off the Pb line (283.3 nm). The slope of the leading edge was 3.3 A s^{-1}. Shorter time intervals between the sample and reference measurements would reduce the errors in Figure 4B in direct proportion (i.e., a time interval of 4.5 ms would result in half the maximum and minimum errors). The errors in Figure 4C–E would be reduced to a lesser extent.

The results obtained for 2% NaCl are consistent with the results obtained using computer modeling and simulated background absorbance. The systematic errors grow smaller as more reference points are used. For most background absorbance problems, the advantage of the quadratic 3 and quadratic 4 modes over the bracketing mode would be hidden in the base-line noise. However, the systematic errors would still be present adding a bias to the results. As in most cases, the size of the analytical signal will determine the significance of the error. For a strong background signal, as shown in Figure 2, the difference in errors can be easily seen.

ACKNOWLEDGMENT

J.A.H. wishes to acknowledge the National Science Foundation's Independent Research Program, which was used for the partial completion of this project.

LITERATURE CITED

(1) Harnly, J. M.; Holcombe, J. A. *Anal. Chem.* **1985**, *57*, 1983–1986.
(2) Savitsky, A.; Golay, M. J. E. *Anal. Chem.* **1964**, *36*, 1627–1639.
(3) Harnly, J. M.; O'Haver, T. C.; Wolf, W. R.; Golden, B. M. *Anal. Chem.* **1979**, *51*, 2007–2014.
(4) Siemer, D. D.; Baldwin, J. M. *Anal. Chem.* **1980**, *52*, 295.
(5) Grobenski, Z., Lehmann, R.; Radziuk, B.; Voellkopf, U. *At. Spectrosc.* **1984**, *5*, 87.

RECEIVED for review April 9, 1986. Accepted July 7, 1986.

Preatomization Separation of Chromium(III) from Chromium(VI) in the Graphite Furnace

Sonja Arpadjan[1] and Viliam Krivan*

Sektion Analytik und Höchstreinigung der Universität Ulm, Oberer Eselsberg, D-7900 Ulm, Federal Republic of Germany

By means of ^{51}Cr as a radiotracer, the behavior of Cr(III) and Cr(VI) in a graphite furnace was investigated. After the addition of a mixture of trifluoroacetylacetone, tetramethylammonium hydroxide, and 0.5 M sodium acetate (1:2:2) to a water or urine sample, Cr(III) can quantitatively be removed from a graphite tube combined with an L'vov platform or from a tungsten-impregnated graphite tube without an L'vov platform at 400 °C while Cr(VI) quantitatively remains in the furnace up to a temperature of 1200 °C.

[1]Permanent address: Clement Okhridsky University of Sofia, Faculty of Chemistry, 1, A. Ivanov, Blvd., Sofia 1126, Bulgaria.

In certain environmental samples, chromium can occur as chromium(III) and chromium(VI). While there is little conclusive evidence on toxic effects of trivalent chromium and it is considered to be essential in nutrition and for the maintenance of normal glucose tolerance, many toxic effects including carcinogenicity have been reported for hexavalent chromium (*1–4*). For this reason, the separate determination of chromium(II) and chromium(VI) in environmental samples has become very important. The concentration of Cr(VI) in urine may be an indicator of human exposure to hexavalent chromium compounds (*5*).

Van Loon et al. (*6*) and Naranjit et al. (*7*) described the

0003-2700/86/0358-2611$01.50/0